MODELLING ULTRASONIC INSPECTION OF ROUGH DEFECTS

J.A. Ogilvy
UKAEA,
Theoretical Physics Division
HARWELL Laboratory
Didcot, Oxon
OX11 0RA, U.K.

INTRODUCTION

Ultrasonic signals are affected by the nature of the defects under investigation. One defect property known to alter signal amplitudes and pulse shapes is surface roughness. No exact theory is available to describe the interaction of ultrasonic waves with rough defects but approximate theories are of great value, over various regimes of validity [1,2]. We have combined one such approximation, Kirchhoff theory [1,2], with many aspects of a real inspection system, to provide a model for simulating the ultrasonic inspection of randomly rough defects. The model is currently acoustic, such that mode conversion effects cannot be predicted. This paper presents some details of the model, together with sample results. These include a comparison with experimental measurements from rough surfaces, showing favourable agreement.

We show how roughness can increase or decrease defect detectability, depending on the inspection geometry. We also show that roughness can lead to difficulties for amplitude based and time based sizing techniques, through loss of definitive signals from which to measure dB drops and loss of distinct diffracted signals from which to make timing measurements.

THE MODEL

Geometry

The model geometry is shown in figure 1. A defect of specified dimensions and orientation is at some depth D below the inspection surface. The roughness of the defect is specified through the r.m.s. height and the correlation length. The transducer parameters are also given as input to the model, including beam angles, crystal radii, centre frequencies and pulse shape. A specified scan is then simulated, calculating the received pulse shape for each scan position along the surface. The received pulse shape may be examined, or the peak amplitude determined. In this manner A, B or C-scan information may be built up. A range of geometries may be specified, including Pulse-Echo, Tandem and Time-of-Flight.

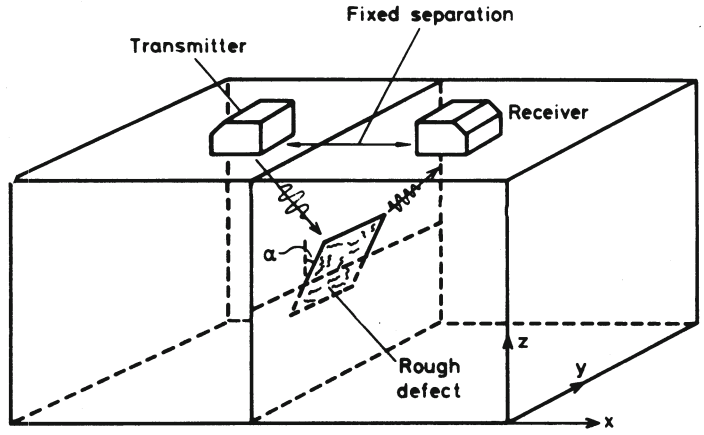

Figure 1. Model geometry.

Surface roughness.

The method of surface generation is described in detail in reference [3] and will only be outlined here. The theory has been extended since that reported in reference 3 to allow for surfaces which are either corrugated or rough in two orthogonal directions. For simplicity we describe here the basics of the method for corrugated surfaces. A set of *uncorrelated* random data, v_i, is first generated, with a Gaussian distribution of zero mean and a given r.m.s. value, σ_v. This data is then correlated by performing a moving average [4], given by:

$$z_j = \sum_{i=-M}^{M} w_i v_{i+j}, \tag{1}$$

where the w_i are a set of weights. The form of the weights chosen for this moving average determines the correlation function of the final *correlated* random data. We have chosen to generate surfaces with Gaussian correlation functions, this being a reasonable smoothed approximation to many measured correlation functions [5]. The r.m.s. height of the rough surface, σ, is then given by [4]:

$$\sigma^2 = \sigma_v^2 \sum_i w_i^2. \tag{2}$$

This method of surface generation allows us to pre-define surface statistics, such that many surfaces of different statistics may be generated to study the effects of varying surface roughness. Furthermore, many surfaces of the same statistics but different profiles, i.e. *realizations*, may be generated to give information on the statistics of the scattered field.

Calculation of scattering at the surface

Acoustic Kirchhoff theory [1,2] is used to approximate the field scattered from a rough surface. Each surface point is assumed to scatter as though it were part of an infinite plane

surface parallel to the local surface tangent at that point. This approximation is exact only for infinite smooth surfaces but remains good for many rough surfaces. We assume the rough surfaces obey Dirichlet boundary conditions, $\psi(\mathbf{r}) \equiv 0$, where ψ is the total wave field. Kirchhoff theory is substituted into the Helmholtz scattering formula to give the far field scattered wave in terms of an integral over the rough surface of the form:

$$\psi^{sc}(\mathbf{R}) = 2i\int_S A(\mathbf{k}_i,\mathbf{r})\mathbf{n}(\mathbf{r})\cdot\mathbf{k}_i\psi^{inc}(\mathbf{r})\frac{e^{ik|\mathbf{R}-\mathbf{r}|}}{4\pi|\mathbf{R}-\mathbf{r}|}dS(\mathbf{r}). \tag{3}$$

In equation (3) $\mathbf{k}_i$ is the incident wavevector and $\mathbf{n}$ is the unit inner normal to the surface at point $\mathbf{r}$. $A(\mathbf{k}_i,\mathbf{r})$ is the amplitude of the incident wave of wavevector $\mathbf{k}_i$ at surface point $\mathbf{r}$ and $\psi^{inc}(\mathbf{r})$ is the incident wave at $\mathbf{r}$ for a spherically spreading source of unit amplitude. This equation represents the summation over the surface of secondary source points.

This integral is evaluated by dividing the rough surface into many small, planar, rectangular 'integration regions' oriented parallel to the local surface tangent. This integral may then be evaluated analytically. The contributions from each of these regions are then summed, to determine the overall scattered field. Reference 6 gives more details.

Other model parameters

To simulate an inspection scan it is necessary to include the directivity and receptivity of the transducers, together with their frequency responses. In the model the transmitter may emit either an infinite wavetrain of single frequency or a pulse of specified shape. If the calculation is time dependent then the pulse shape $f(t)$ is specified along the beam axis. The Fourier transform of the pulse, $F(\omega)$, then gives the amplitude of each frequency component along the beam axis. To take account of the variation of beam spread with frequency a beam amplitude profile is assumed, of the form:

$$A_i(\Theta) = \frac{J_1(ka\sin\Theta)}{ka\sin\Theta}. \tag{4}$$

Θ is the angle from the beam axis, $J_1(x)$ is the first order Bessel function of the first kind, a is the transducer crystal radius and k is the wavevector modulus. The amplitude of any frequency component incident onto a small integration area is then determined by $F(\omega)$, together with equation (4). The receptivity of the receiver is calculated using an expression of the form of equation (4). The relevant phases are calculated from knowledge of the ranges to and from the transducers, assuming spherically spreading waves.

To calculate the received pulse at any scan position the incident wave amplitude and phase is calculated for each integration area, over the range of frequencies within the pulse. By summing the contributions from all the areas, for each frequency, and taking account of the receiver receptivity, the received amplitude is determined for each frequency. The inverse Fourier transform gives the received pulse, with the peak amplitude of this pulse giving the scattered amplitude. For a monochromatic calculation a single summation is carried out, at the appropriate frequency, giving a value for the scattered amplitude. Full details of the workings of the model are given in reference 6, together with some results from the model.

Several comparisons of the model predictions with experiment have been made, and these are reported in reference 6. Figure 2 shows results from one such comparison. Here Pulse-Echo signal amplitudes are given, as a function of angle of incidence, for surfaces of three levels of roughness. In each case the signals are normalised relative to the results for normal incidence. The experimental measurements are shown as crosses and the model predictions as solid circles. Each data point is an average over four different realizations. The experimental results are taken from reference 7. There is excellent agreement between the model and experiment, except for the roughest surface, for which Kirchhoff theory is not expected to be good.

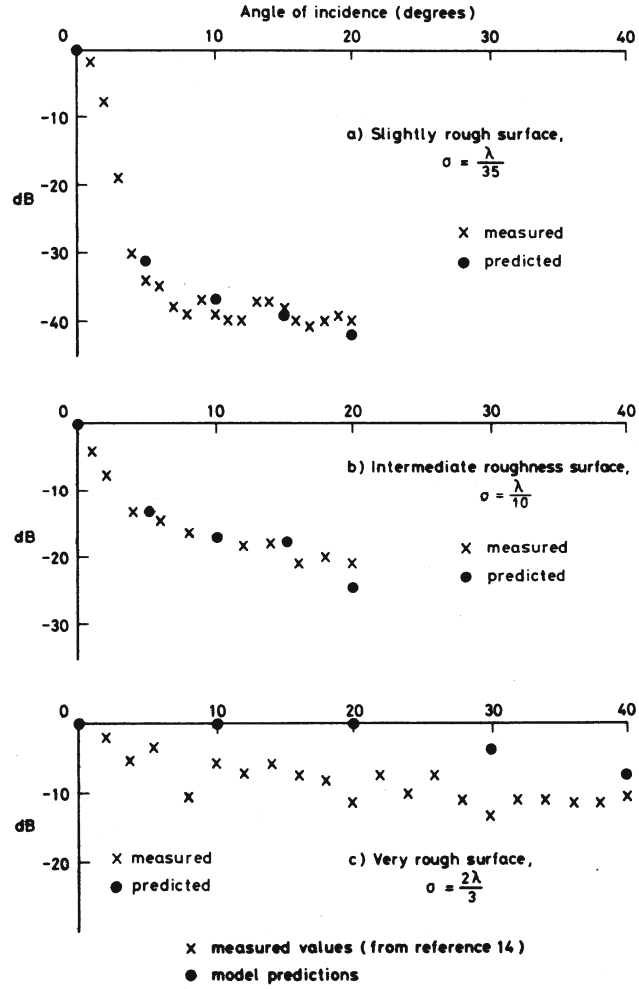

Figure 2. Variation of Pulse-Echo signal with angle of incidence. Note the good agreement between the model predictions (●) and the experimental results (×, from reference 7), except for the roughest surface, where Kirchhoff theory may not be good.

DEFECT DETECTABILITY

The detectability of a defect may be enhanced or reduced by the presence of roughness, depending on the inspection geometry. Figure 3 shows results from the model for 45° scans across defects of various roughnesses, for vertical defects and defects tilted by 20° and 45°. The inspection geometry is shown in figure 3a. For defects tilted by 45° the specular signal is detected. Roughness therefore diminishes the received signal and hence reduces detectability, as seen in figure 3b. However, beyond some level of mis-orientation defect detectability is enhanced. This is seen in figure 3d, where the rough vertical defects lead to higher signals than smooth defects of the same orientation. Defect detectability is therefore enhanced, because of the widely scattered diffuse field from rough defects, this exceeding the small off-specular field from smooth defects.

DEFECT SIZING

Defect sizing using amplitude based or time based techniques is affected by roughness. Amplitude based techniques using dB drop measurements rely on the decrease in signal amplitude which occurs when scanning across a smooth defect, as the beam reaches the defect edge. Measurement of dB drop is then taken from the central constant 'plateau' amplitude and used for sizing. For rough defects this plateau amplitude no longer exists, from which to take timing measurements. This is clearly seen in figure 4, where 0° Pulse-Echo scans are simulated, where the defect extent is greater than the beam width at the defect. The loss of the constant plateau signal is apparent.

Surface roughness can also affect timing measurements: for successful sizing of a defect using time measurements two distinct signals are required, these arising from the top and bottom edges of the defects. This can usually be obtained for smooth defects. Figure 5a shows an example of the pulse received from a smooth defect using 60° Pulse-Echo inspection, according to the model. Two distinct signals are recorded, with their separation determined by the size of the defect and the wavespeed. Figure 5b shows an equivalent result from the model, for a rough defect. The two distinct signals have been lost, since scattering now occurs from the whole defect face, such that energy is received at all times between the start of the diffracted signal from the nearer defect edge and the end of the diffracted signal from the further edge. Timing measurements would be difficult from such a signal.

SIGNAL SPREADS

Each rough surface scatters differently from any other rough surface, even if their statistical parameters are the same. Such surface realizations will therefore lead to a spread in expected signal amplitudes, for any specified level of roughness. This model may be used to determine this expected spread, for any inspection geometry and level of roughness. Figure 6 shows results from 45° Tandem scans of 5 rough vertical defects of r.m.s. heights $\lambda/5$. The spread in signal amplitudes is around 8dB for this level of roughness. This spread will vary according to the inspection parameters but is quite typical of the model's time-dependent predictions. Signal spreads are larger for monochromatic wave scattering, although such predictions are less realistic from the practical NDT viewpoint.

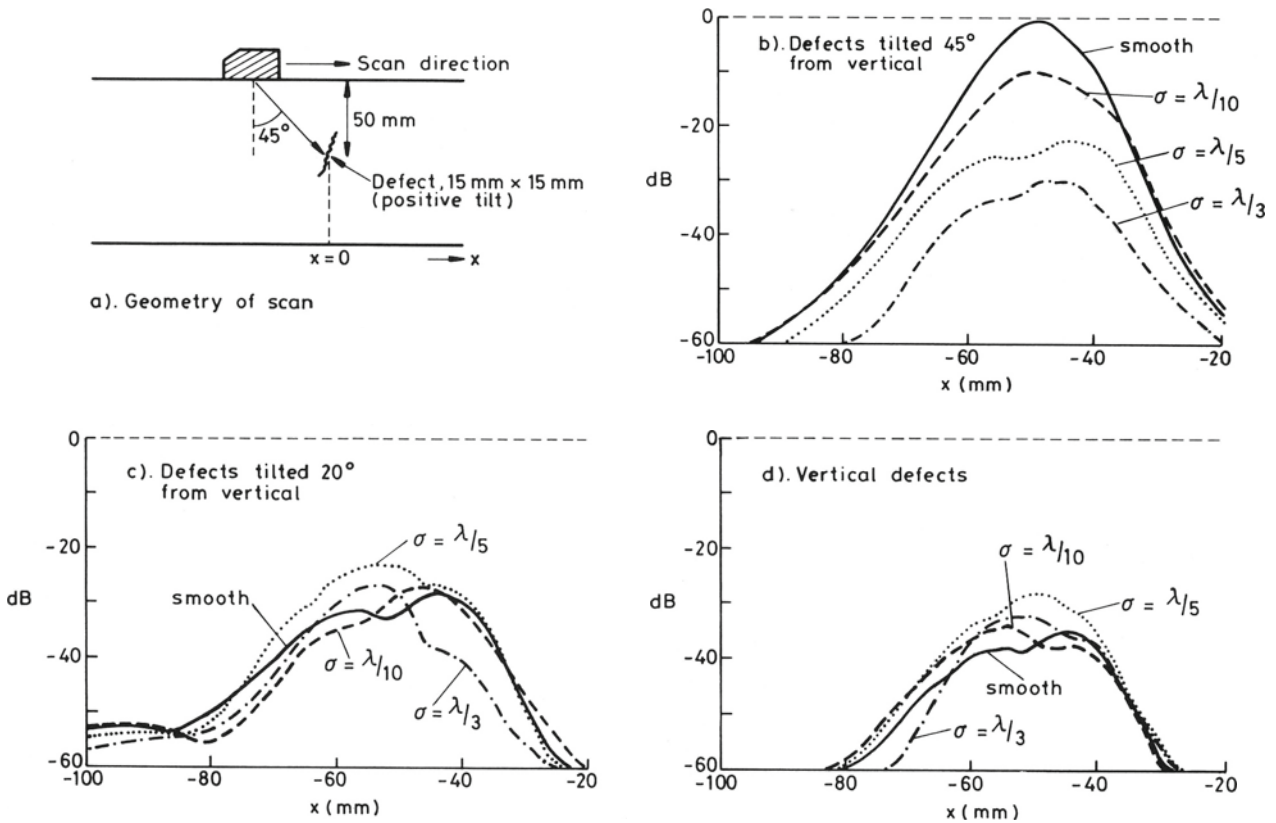

Figure 3. Predicted 45° pulse-echo signals for a 2MHz pulse, 6 cycles long. Increasing roughness decreases the specular signal (as shown in (b)) but can increase the off-specular signals (as shown in (d) and (e)).

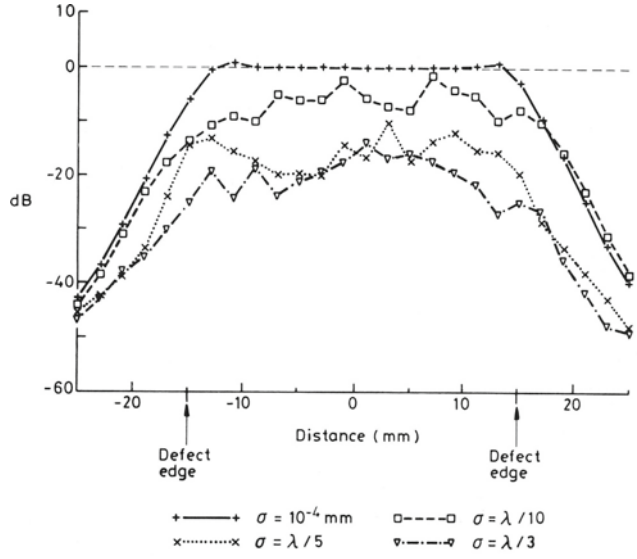

Figure 4. Predicted scan variation as a function of roughness, for 0° pulse-echo inspection of horizontal defects. The loss of 'plateau signal' from which to measure dB drop is seen. Note the sensitivity of the peak signal to a roughness of $\lambda/5$.

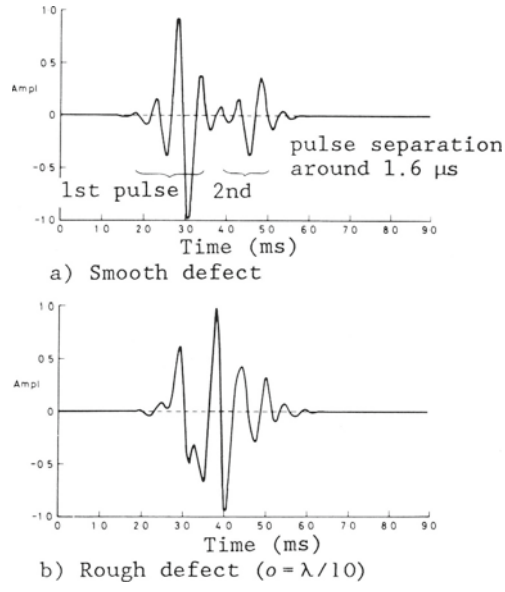

Figure 5. Scattered pulse shapes from smooth and rough defects, showing the loss of distinct diffracted signals from the rough defect because of scattering from the defect face.

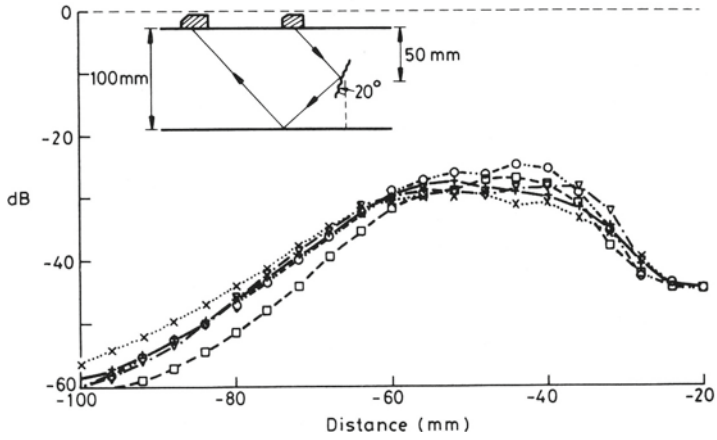

Figure 6. Predicted signal levels from 5 surface realizations, for 45° Tandem inspection of defects, roughness $\lambda/5$. The incident pulse is 2MHz, 6 cycles long. The maximum signal spread is about 8dB.

CONCLUSIONS

A model has been described for studying the effects of surface roughness on ultrasonic signals. The model combines many aspects of inspection systems with a theory for the interaction of waves with rough surfaces, to give realistic predictions. The model is currently acoustic, such that effects arising from mode-conversions cannot be simulated.

The model has been used to show how roughness can alter the pattern of ultrasonic signal amplitude received during a scan. This has been related to changes in defect detectability and sizing arising from the presence of defect surface roughness. Signal spreads can also be predicted, as the model allows for the study of scattering from many surface realizations of the same statistical parameters.

REFERENCES

1. P. Beckmann, A. Spizzichino. The scattering of electromagnetic waves from rough surfaces. Pergamon, (1963).
2. F.G. Bass, I.M. Fuks. Wave scattering from statistically rough surfaces. Pergamon, (1979).
3. J.A. Ogilvy. Computer simulation of acoustic wave scattering from rough surfaces. J. Phys. D: Applied Physics, 21(2), 260-277, (1988).
4. C. Chatfield. The analysis of time series: theory and practice. Chapman and Hall, (1975).
5. D.J. Whitehouse, M.J. Phillips. Discrete properties of random surfaces. Phil. Trans., A290(1369), 267-298, (1978).
6. J.A. Ogilvy. A model for the ultrasonic inspection of rough defects. UKAEA report: AERE-TP.1297, May 1988. (HMSO). Also to be submitted to Ultrasonics.
7. M. deBilly, G. Quentin. Backscattering of acoustic waves by randomly rough surfaces of elastic solids immersed in water. J. Ac. Soc. Am., 72(2), 591-601, (1982).